

# Is there a Pulsar in Supernova 1987 A?

A recent announcement of the discovery of a pulsar in Supernova 1987 A in the Large Magellanic Cloud has excited the world-wide astronomical community. New observations at the La Silla Observatory by a group of European astronomers<sup>1</sup> from the Max Planck Institute for Extraterrestrial Physics and the European Southern Observatory, however, do not confirm the reality of this object. More observations are now needed to settle this important question.

## Searching for the Pulsar in Supernova 1987 A

Since the explosion of the now famous supernova in the Large Magellanic Cloud on February 23, 1987, astronomers have been eagerly waiting for the emergence of a newborn *pulsar*. Current theories predict that the explosion of a heavy star as a supernova will result in most of its mass being blown out into surrounding space, but also that some of it will be compressed into an extremely dense and rapidly rotating *neutron star* at the centre. Such an object would later manifest its presence in the supernova by the emission of regular light pulses (hence the name "pulsar"). Neutron stars measure no more than 10–15 kilometres across, but they weigh as much as our Sun which is about 100,000 times as large.

Of half a dozen pulsars known in supernova remnants, the most famous are those in the Crab Nebula and the Vela Nebula. The detection of a pulsar inside SN 1987 A, the first naked-eye supernova in nearly four centuries,

<sup>1</sup> The group consists of Hakki Ögelman, Günther Hasinger and Wolfgang Pietsch (Max-Planck-Institut für Extraterrestrische Physik, Garching bei München, F. R. Germany), Christian Gouiffes, Jorge Melnick, Thomas Augusteijn, Flavio Gutierrez, Preben Grosbøl and Christian Santini (ESO) and Holger Pedersen (formerly ESO, now Nordic Optical Telescope Scientific Association).

would provide the definitive confirmation of the creation of pulsars in supernova explosions. Extensive searches for such a pulsar have therefore been made at some southern observatories since the explosion was first recorded, almost exactly two years ago. This is done by observing the supernova light with a "rapid" photometer, capable of measuring the light intensity many times each second. A pulsar would reveal itself by the presence of brief "flashes" of extra light, regularly spaced in time.

Immediately after the explosion, the dense cloud around the supernova did not allow a look at its centre, but as the clouds become thinner, light from the new pulsar should eventually become visible. Many astronomers have been waiting for this exciting moment.

## First Detection?

On 8 February 1989, a group of American astronomers<sup>2</sup> announced the discovery of a very fast pulsar in SN 1987 A, flashing no less than 1969 times per second. This is referred to as 1969 cycles/second and supposedly corresponds to the number of rotations per second by the pulsar. No other pulsar has ever been found to rotate this fast. These observations were made on January 18, 1989 at the Cerro Tololo Interamerican Observatory, situated about 100 km south of La Silla. Surprisingly, the American group did not see any pulsations when the observations were continued 12 days later with another telescope.

At the European Southern Observatory, the light of the supernova has been monitored with a special, rapid photometer at the 3.6-m telescope at regular

<sup>2</sup> This group is headed by John Middleditch, Los Alamos National Laboratory; the announcement was made on Circular 4735 of the International Astronomical Union (IAU).

intervals during the past year. The intensity of the supernova light was measured 1000 times per second, a rate which was determined from theoretical considerations about how fast the predicted pulsar in SN 1987 A might rotate. However, it is too slow to show variations at the rate observed at Tololo.

## New Observations Fail to Provide Confirmation

In order to confirm the presence of a pulsar with the higher pulsation rate, the ESO instrument was modified immediately after the announcement by the American group, so that it can now measure the supernova light up to 10,000 times per second. On February 14 and 15, observations were performed at the 3.6-m telescope during a total of 8 hours. The data tapes were rushed to the ESO Headquarters in Garching near Munich. The detailed results of a careful analysis at the Max Planck Institute for Extraterrestrial Physics have now been published on IAU Circular 4743 (24 February 1989).

The European team finds that no pulsating signal is present in the ESO data near 1969 cycles/second, to a limit of 1/4000th of the intensity of the supernova light. Nor is there any obvious signal at any other frequency in the interval from 1 to 5000 cycles/sec. These observations therefore do not provide confirmation of the presence of a pulsar.

If there is a pulsar in SN 1987 A, then the absence of observed pulsations in the measurements obtained after January 18, both by the American and the European groups, possibly indicate that the pulsar is being intermittently obscured by dust clouds around the supernova.

Further observations will therefore be needed to definitively demonstrate the reality of a pulsar in Supernova 1987 A.

(From ESO Press Release 02/89,  
24 February 1989.)

# Squeezing the Most from the CES

H. BUTCHER and T. SCHOENMAKER, Kapteyn Observatory, Roden, the Netherlands

## Introduction

In the *Messenger* No. 51 (p. 12–15), an attempt to use the CES for radioactive chronometry of the Galaxy was described. Two instrumental aspects of the observations were noted as being not yet under adequate control: (i) The

determination in detail of the instrumental profile, the wings of which cannot be determined well, except at laser line wavelengths, and the shape of which is found to depend on the often variable focus across the array detector format, and at least sometimes on the signal

level in the detector used. (ii) The markedly asymmetrical distribution of the noise from the Reticon detector (caused by energetic particle detections) for low flux levels and integrations of an hour and longer. Treatment of the data in an optimum way is problematical due to

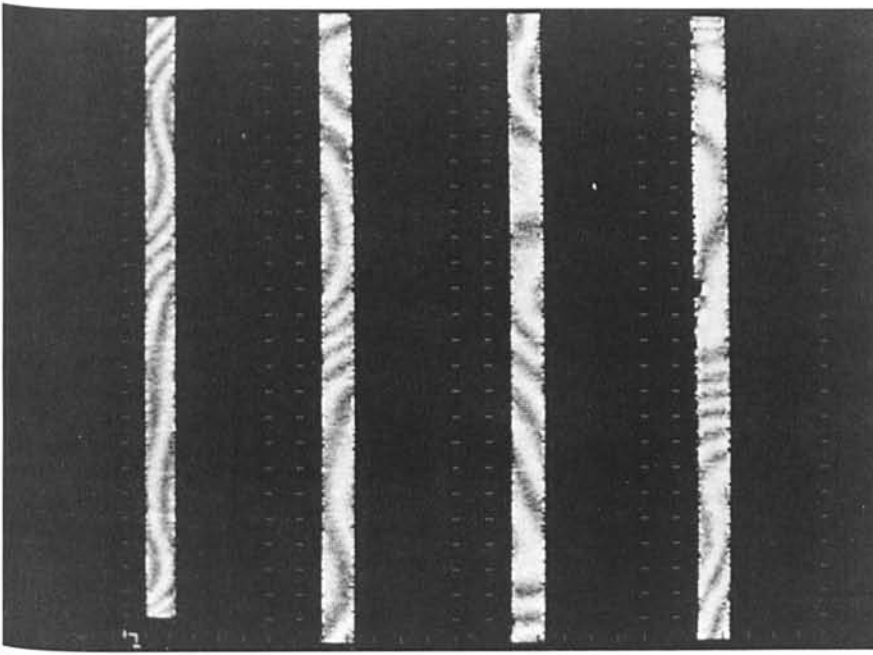


Figure 1: Flat field correction frame displayed in four segments, starting at lower left and finishing at upper right. The frame has a mean correction of 1.000, with fringes and small scale sensitivity variations visible as deviations from 1.0 wherever there is sufficient signal for meaningful correction.

these effects, and although the CES remains one of the world's best instruments of its type, study of such deficiencies can be expected to improve its performance significantly.

A satisfactory way of deriving the instrumental profile is, to our knowledge, still lacking, but with the possibility of using the new double density RCA CCD on the long camera, it seemed possible to substantially improve the noise characteristics of the data. That is, one can image the spectrum so that each spectral channel covers several pixels, and discriminate and eliminate (mostly single pixel) particle detections during data reduction. When Daniel Hofstadt on La Silla was approached in late 1987 about when this detector might be available to long-camera users, he graciously promised to help provide it for a CAT/CES run on 15–22 April 1988 – but only if a detailed report of the experience would be prepared! This article is adapted from that report.

The CCD we used was ESO CCD No. 9, an RCA SID 503 high resolution, thinned and backside illuminated device, with  $1,024 \times 640$ , 15 micron square pixels. We used a data format of 1,030 rows of 61 pixels each, with the spectrum recorded along the long dimension. The noise is quoted at 40 electrons rms when used in the fast readout mode. We decided to use the slow readout mode, however, for which we could discover no precise noise figure; our data are consistent with a system noise of about 35 electrons rms. The dark

current was said to be 2.5 electrons per pixel per hour, a value which agrees with our data. The charge transfer efficiency was reputed to be very good for this chip. Our spectral lines were all in the blue region, near  $4000 \text{ \AA}$ , and we were pleased to discover that the overall detection efficiency at this wavelength was very reasonable. A bad column was present near the centre of the chip, but our sub-format could be set up to avoid it. The spectrum signal showed a roughly gaussian shape in horizontal profile, some 5 pixels FWHM for the stellar data and 8 pixels for the calibrations.

All things considered, this chip seems to be representative of the higher quality devices available to astronomers today, and we were particularly interested to determine what the limits of its photometric performance would be.

## Analysis

To try to extract stellar spectra in an optimum way from the 2-D CCD data, we have used the following processing steps.

### (1) Background subtraction and flat fielding

We use a constant for the background, because all our dark frames were beautifully uniform and flat. We had three kinds of flat field data: continuum light from the internal calibration lamp, from a rapidly rotating hot star observed under similar circumstan-

ces to our programme stars, and from an illuminated patch on the inside of the dome observed through the telescope. Unfortunately, the intensity of the dome flat field was never sufficient in the blue to allow adequate S/N to be achieved. The other two sources yielded very similar results: the spectra, even at  $4000 \text{ \AA}$ , show fringing at the 5% level, but luckily this fringing is rather stable and we could not really distinguish between internal lamp data and the stellar spectrum for this purpose.

We prepared the flat field correction by heavily smoothing the continuum spectrum in the direction of dispersion, then dividing the raw spectrum by the smoothed one, to yield a flat correction picture with data values near 1.0. For those parts of the frames where the signal is so low that this procedure would objectionably amplify the noise, or where division is by nearly or exactly zero, we simply replace the ratio value by exactly 1.000. This correction picture is then divided into the data frames, removing high frequency sensitivity variations and fringes, while leaving the low frequency echelle order intensity envelope unchanged. An example of the resulting flat field correction frames is shown in Figure 1. Again the fringes have peak-to-peak amplitudes of roughly 10%, and in places are of such a spatial frequency and orientation that they could cause significant line strength errors without obviously being seen to do so.

### (2) Extraction of one dimensional spectra

Because we want to maximize the final S/N in our extracted spectra while minimizing the effects of particle detections and single pixel defects, we choose to derive a template function in the direction perpendicular to the spectral dispersion, and fit this function by iterative least squares at each position along the spectrum.

The template is derived by averaging on the order of a hundred rows of data (each row consisting of 61 pixels cutting across the spectrum), selected from the centre region of the format so as to avoid obviously bad pixels. A typical template is shown in Figure 2a. This averaging process ensures not only that the S/N of the template signal is much higher than that of the data to be fitted, but also that it represents an average signal strength in the data at hand, and hence should suffer minimally from any photometric non-linearities present.

Our fit of the non-analytical templates to the data assumes that three parameters are involved: a (flat) background level, a multiplicative gain factor for in-

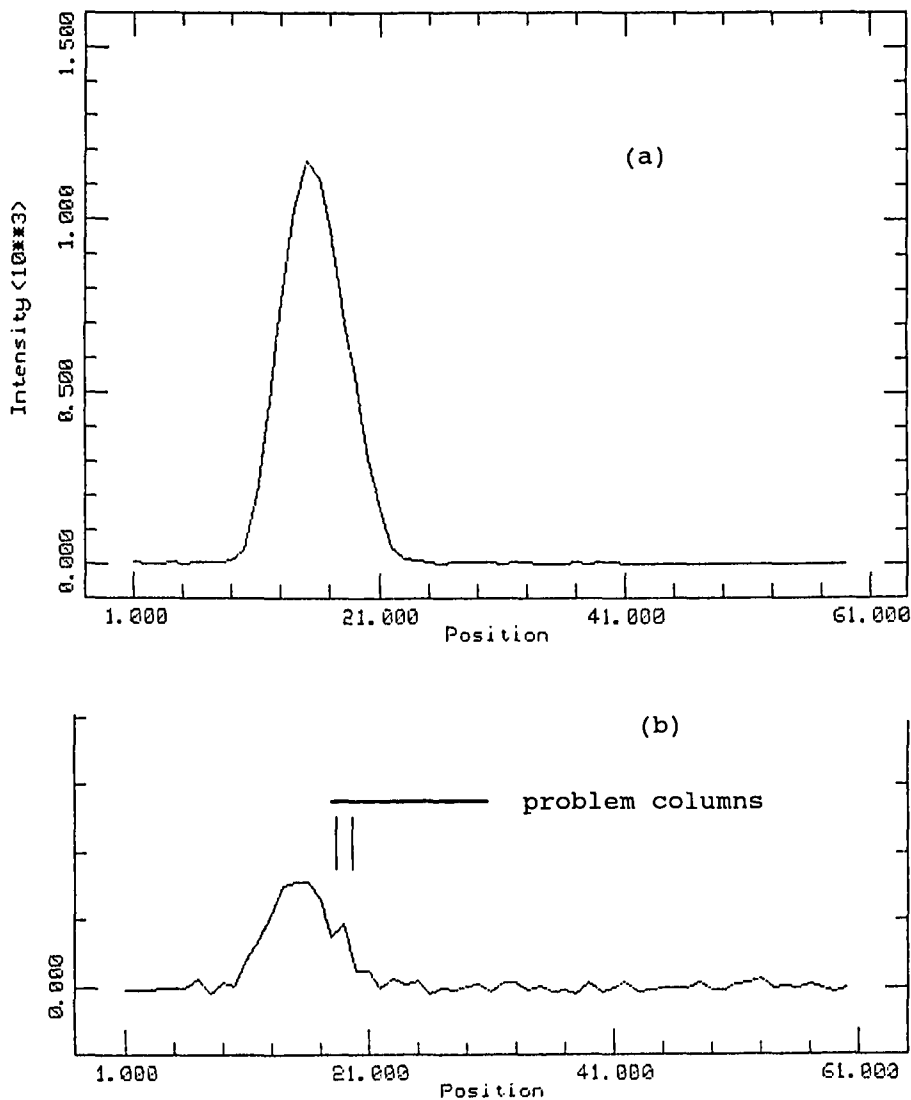


Figure 2: (a) Typical signal template, used for fitting to each spectral channel. (b) Trace of data perpendicular to spectrum in the bottom of an absorption line, showing anomalous columns.

tensity, and a shift in the x coordinate (i.e., perpendicular to the spectrum). At each channel (y position) along the spectrum we fit the template, calculating the derivative of the template with respect to the x coordinate using fifth order polynomial interpolation. The rms difference between the template and data is minimized by iterating until the calculated parameter changes are no greater than those expected from the *a priori* known noise, or until a maximum number (usually 7) of iterations has been made. For reasons sketched below, it has been found necessary to apply a mask to eliminate some of the data from the fitting process.

### (iii) Wavelength scale and continuum correction

Finally, we have used the internal thorium lamp at the CES to obtain a wavelength calibration, and have extracted a spectrum from the (fringe

corrected) flat field continuum data to provide a first correction for the large-scale sensitivity and echelle order varia-

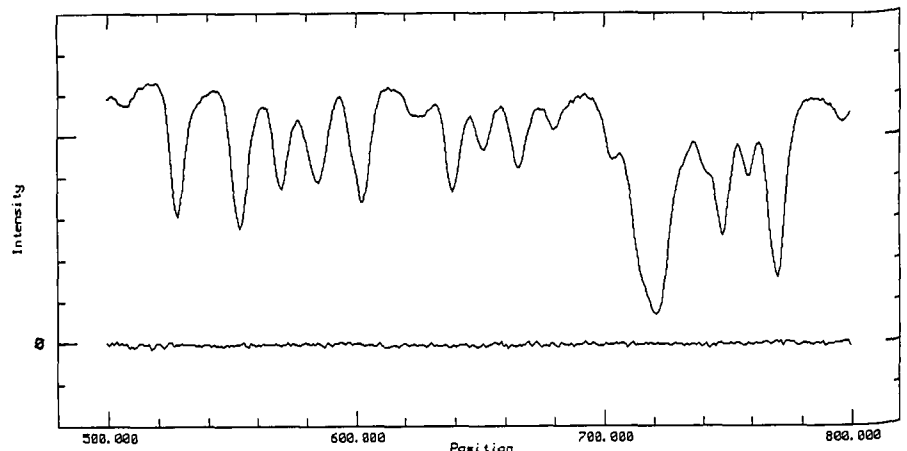


Figure 3: Extracted spectrum from a single, well-exposed spectrum of a solar type dwarf star. The spectral resolution is 100,000. The strong absorption line at pixel position 720 is Fe I 4132 Å. The noise trace near zero intensity is the subtraction of two such spectra, which differ in recorded signal level by 30-40%.

tion along the spectra. As have other workers, we find that the scatter around the fit of the thorium emission lines is rather larger than estimated from the noise in the data. The resulting wavelength scale is adequate for our purposes, but it is clear that future calibration facilities for such high quality spectrometers should incorporate a solid Fabry-Perot etalon, to yield many sharp lines with precisely known spacings for the dispersion calibration.

We also note that our thorium calibration data show wavelength zero point jumps during one night of up to 1.9 km/s. We do not know the origin of these jumps, but evidently for radial velocity programmes it is important to take wavelength calibration spectra at regular intervals with the CES.

Assigning a temperature to the internal lamp spectrum of 2,800 K and ratiating it to a black body spectrum at that temperature yields a correction to the large scale sensitivity variations from one end of our spectra to the other which we estimate are accurate to better than 10%. The main uncertainty arises because of the differing optical paths of stellar and lamp light in the instrument, which in principle can give rise to illumination differences of the optics. At least to first order, however, this strategy provides a useful correction.

## Results

In Figure 3 is shown a processed spectrum of a 3.6-mag star, from an integration of 15 min, and the difference between it and a second integration of the same star immediately following. The signal levels in the two cases differ by more than 30%, due to variable seeing. It is evident that the fitting procedure automatically normalizes all spec-

tra to a common intensity scale (no scaling in intensity was made here), and that there is no significant detector non-linearity present (which would be manifest as residual differences at the positions of strong lines). Furthermore, the difference of the spectra has an rms noise very near to the calculated photon shot noise limit, given the quoted 6.8 electron/ADU calibration.

From these and other results from the run it is clear that apparent S/N ratios of 300 : 1 are achievable with this detector. Higher ratios may be possible with multiple integrations.

The only serious problem found in our data is shown in Figure 2b. The two columns marked there consistently show residuals (data-minus-fit) dependent on signal level. We understand (Sandro D'Odorico, private comm.) that these RCA chips are known to exhibit such behaviour – that is, to have occasional column pairs in which part of the signal in one column seems to end up in the adjacent column, when the signal is above some threshold level. We have experimented with trying to fix this problem by applying an interpolated re-transfer of signal after the fact, but could not convince ourselves that the results were always reliable.

Our solution to the problem is to mask the offending columns of data away, and exclude them from the template fitting process. We thereby lose some 15% of our signal, which we deem an

acceptable loss to guarantee the quality of the photometry. The data in Figure 3 were processed with these columns masked away.

One negative side effect results, however. With two fewer signal columns, the fitting algorithm now no longer effectively ignores the single pixel outliers due to particle detections. We have had to include a routine, therefore, to test for pixels more than 5 times the (*a priori* known) noise sigma from the fit, and throw the worst single one out. Although not particularly elegant, this strategy has proven very effective in removing particle detections.

### Focus Effects

Our data-minus-fit residual frames are exquisitely sensitive to focus variations along the spectra (although the final integrated intensities at each point should not be). We find that the width of the spectra does vary, being broadest at the two ends, but that the effect is so small that we cannot measure it in the widths of individual emission lines in the calibration spectra. We suppose that a small tilt of the CCD with respect to the focal plane of a half degree is sufficient to give the magnitude of what we see. From the residual frames we infer that over about a quarter of the total length of the recorded data, the instrumental profile is clearly constant enough for use

in spectral modelling analysis with a single model profile. But of course, the derivation of the appropriate profile remains problematical.

### Conclusions

Based on our, admittedly incomplete, analysis, we feel we can make the following conclusions.

(i) The double density RCA CCD on the CES long camera works very well, even at 4000 Å.

(ii) Its lower noise per pixel compared to the Reticon, and its registry of each spectral channel with multiple pixels, allows particle detections to be discovered and easily removed.

(iii) The expected quantum noise limit is achieved on single integrations, allowing S/N ratios of several hundred to be obtained. We have not done tests to determine whether S/N ratios of 1,000 and greater are possible, by summing multiple integrations.

(iv) Photometrically unacceptable columns on the detector have been discovered, which should be masked out during analysis if results of the highest quality are to be attained.

(v) Least squares fitting of templates for data extraction, and probably also for wavelength calibrations, seems a good way to determine the length of spectrum over which the instrumental profile is sensibly constant in shape.

## What is the Mass-to-Light Ratio of the Old Magellanic Globular Cluster NGC 1835?

G. MEYLAN, ESO

P. DUBATH, M. MAYOR, Observatoire de Genève, Switzerland, and

P. MAGAIN, Institut d'Astrophysique de Liège, Belgium

### 1. Richness of the Southern Sky

We astronomers are lucky: our Galaxy has two companion galaxies, the Large and Small Magellanic Clouds, situated well above the galactic plane, which contain a huge potential of astrophysical information. For example, concerning star clusters, the realm of the globular clusters is much richer and more varied in the Magellanic Clouds than in the Galaxy: rich clusters of all ages are observed, from the youngest, having ages of a few tens  $10^6$  yr, to the oldest, having ages of the order or larger than  $10^{10}$  yr. In this paper, only old Magellanic and galactic globular clusters are considered.

From the determinations found in the literature of the individual masses of the richest old clusters, a systematic difference seems to exist between the globulars in our Galaxy and in the Magellanic Clouds, Magellanic clusters appearing lighter than galactic clusters. This difference in mass between old rich Magellanic and galactic clusters obviously has direct consequences on the mass-to-light ratio determination of the considered clusters, reflecting perhaps systematic differences in mass function. This was challenged and discussed recently (Meylan 1988b). A way to resolve this controversy consists in obtaining good observational values of the central

velocity dispersion, by detecting the very small line broadening present in the integrated light spectra.

### 2. Magellanic and Galactic $M/L_v$ Ratio

#### 2.1 Magellanic globular clusters

The method most often used for obtaining the total mass of Magellanic clusters is related to the systemic rotation of the Magellanic Clouds. The observed value of the tidal radius  $r_t$  of the cluster is transformed into mass, in a way similar to the case of galactic open clusters. It is assumed that the clusters